Vibrotactile cues with net lateral forces resulting from a travelling wave

Mondher Ouari[1 [0009−0006−4767−9067]], Anis Kaci[1 [0000−0001−9405−6037]], Christophe Giraud-Audine[1 [0000−0003−3461−0328]], Frederic Giraud[1 [0000−0002−5688−711X]], and Betty Lemaire-Semail[1 [0000−0002−4157−6976]]

Univ. Lille, Arts et Métiers Institute of Technology, Centrale Lille, Junia, ULR 2697 - L2EP, F-59000 Lille, France

Abstract. Ultrasonic travelling waves possess the capability to induce net shear forces on the finger pulp, which finds utility in various applications. This study specifically investigates their potential in generating vibrotactile cues through force modulation. Two experiments are outlined herein. In the first, we assess the detection threshold, estimated at 1.5 µm peak-peak for a modulation frequency of 75 Hz. Remarkably, this threshold closely aligns with that observed in conventional vibrotactile indentation and remains consistent regardless of the force modulation method employed. In the second experiment, we correlate the amplitude of a travelling wave tactile display with the vibration amplitude of a shaker to achieve equivalent vibration intensity. Our findings reveal a substantial amplitude ratio range experienced on the travelling wave device, spanning from 24 to 155, which is pivotal in optimizing vibrotactile stimulator design. Additionally, we demonstrate that vibrations below 1 µm yield negligible net lateral forces on the finger pulp. These results underscore the potential of ultrasonic travelling waves in enhancing tactile feedback systems.

Keywords: Vibrotactile, travelling wave, haptic display, ultrasonic vibration, Net lateral force.

1 Introduction

Tactile cues can be conveyed to users through vibrations generated by actuators in contact with the skin, leading to the development of advanced human-computer interaction systems. For example, button clicks can be simulated using electromagnetic [20] or piezoelectric [13] actuators, inducing vibrations on touchscreen displays. Additionally, modulation of vibration patterns enriches user interaction [6, 17]. Notably, vibrations can be delivered either in the normal [7] or tangential [19] directions relative to the contact area. Perceptually, sensitivity is higher and more stable for tangential vibrations compared to normal ones [15, 2].

A new generation of tactile actuators capable of producing net shear forces on the skin has recently emerged. These actuators employ techniques such as

asymmetric friction combined with high-frequency ultrasound [4], elliptical motion of particles induced by travelling waves [10, 3], and modal superimposition [8]. Travelling waves and modal superimposition generate net shear forces by inducing elliptical motion of particles on a plate or a ring at ultrasonic frequencies [11]. In both cases, two vibration modes are excited with a $\pm 90°$ phase shift.

Previous studies on the elliptical motion of particles predominantly focused on the fingertip as the location for force generation. For instance, authors in [10] observed a decrease in force with increasing finger velocity, while [4] noted force occurrence even with a fixed finger.

Travelling wave stimulators offer the advantage of producing low-frequency vibrations (below 1kHz) with minimal displacement (around 1 µm), ideal for creating vibrotactile patterns on the skin. Modulation of net shear force involves mechanisms such as reducing particle rotational speed by decreasing vibration amplitude [10], or adjusting the standing wave ratio (SWR) through phase shift modification [5, 3]. Moreover, reverse motion is achievable by reversing the phase shift from $+90°$ to -90°.

Several applications have been proposed for this type of actuator. For example, [3] aims to create a virtual environment, while [11] achieves a button click sensation by synchronizing the change of direction of the travelling wave with the moment the pressing force exceeds a threshold. This principle was later applied by [8] using modal superimposition on a finite glass plate.

In this paper, we explore the generation of vibrotactile cues using the principle of elliptical motion generated by a travelling wave to stimulate the finger pulp. Devices based on ultra net shear forces have the potential to become more versatile and can offer better haptic feedback by incorporating vibrotactile cues, making this uncharted territory the primary focus of our investigation. Specifically, we investigate how low-frequency vibrations produced by modulated net shear forces can be perceived with the same intensity as normal vibration. To achieve this, we conduct a psychophysical study to determine the minimal detection threshold of vibrotactile cues and compare two methods for modulating net forces to assess sensitivity differences. In the second experiment, participants are tasked with adjusting the level of a normal vibrotactile stimulator to match the intensity of the travelling wave based device.

2 Experimental Setup

The travelling wave is generated by the stator of a Shinsei USR60 ultrasonic motor (Shinsei Corporation, Japan), shown in Figure 1.a, which is composed of a ring to which two sets of piezoelectric actuators are glued. The first set is used to excite a ring bending mode denoted “1” (Figure 1.a), whose resonance frequency is $f = 40kHz$ with a wavelength $\lambda = 21mm$. The second set is used to excite a twin mode denoted by "2" with the same resonance frequency and the same wavelength, but spatially offset by a quarter of a wavelength $\lambda/4$. The two voltages applied to the sets of piezoelectric actuators are generated by a DSP (Digital Signal Processor, nucleo-STM32F446 for STM) which are amplified via

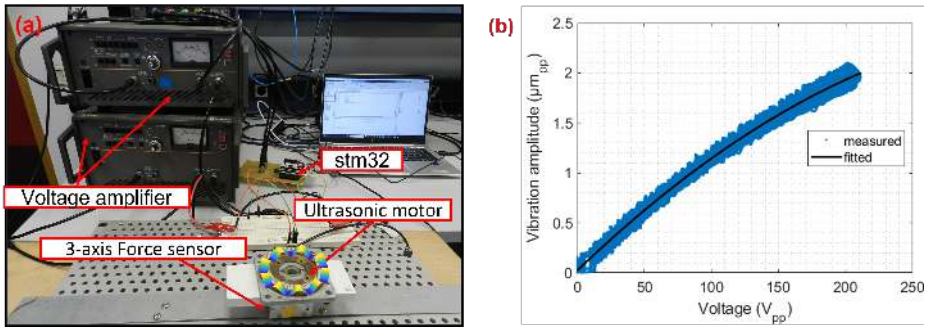

Fig. 1. (a) The experimental setup with the mode shape represented on the USR, (b) Relation between the excitation voltage and the vibration amplitude.

two voltage amplifiers (HSA4051 and HSA4052 from NF JAPAN) to reach up to 300 Vpp. The resulting vibration is written as:

$$w_1(t) = \frac{A}{2} \times cos(2\pi ft) \quad w_2(t) = \frac{A}{2} \times cos(2\pi ft + \phi) \tag{1}$$

with w_1 and w_2 are the deflection of the modes 1 and 2 respectively, A is the vibration amplitude peak to peak and ϕ is the phase shift.

The relationship between the control voltages and the vibration amplitudes of the unloaded device was identified using a laser vibrometer (Polytec OFV 505) and is presented in Figure 1.b for $\phi = 90°$. The curve shows nonlinear behavior, which is taken into account in our study. It is worth noting that the pressing of the finger within the force limits stipulated in this study has a negligible effect on the amplitude.

Finally, a 3-axis force sensor (K3D40 from PM instrument) is mounted under the USR; it monitors the normal force F_N and measures the net lateral force F_L produced by the system.

3 Modulation of the net shear force for vibrotactile cue

With a travelling wave, the elliptical motion of the particles of the stator drives the finger pulp due to frictional mechanisms [16]. The model of this interaction is outside the scope of this paper, but it is generally admitted that the force F_L depends on the vibration amplitude A, the phase shift ϕ, and the pressing force F_N. The two methods are implemented in order to modulate the net shear force, and are illustrated in Figure 2. The first method modulates the vibration amplitude A (AM) and keeps a phase shift $\phi = \pm\frac{\pi}{2}$. In this way, the travelling wave is maintained, but its amplitude is modulated. The second method keeps a constant vibration amplitude A but modulates the phase shift $-\pi \leq \phi \leq \pi$ (PM). This will modify the standing wave to travelling wave ratio. In the paper, sinusoidal modulations at frequency f_{LF} with vibration amplitude A_0 are used, and we have:

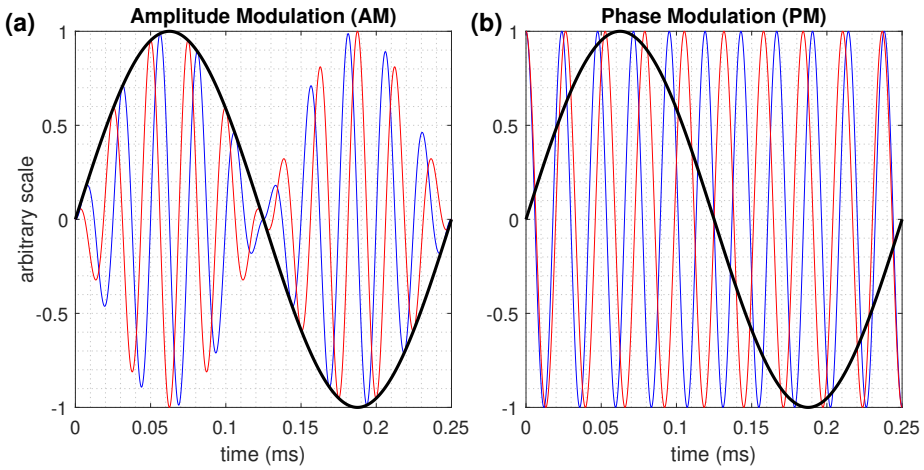

Fig. 2. Proposed methods of modulation, the frequencies are not in scale, they were chosen for illustration. w_1 in blue, w_2 in red and the reference signal in black : (a) Amplitude modulation and (b) Phase modulation.

- Amplitude Modulation (AM): $A = A_0 \times \sin(2\pi f_{LF} t)$, $\phi = 90°$
- Phase Modulation (PM): $A = A_0$, $\phi = \frac{\pi}{2} \times \sin(2\pi f_{LF} t)$

Since the force generation relies on friction mechanisms, nonlinear behavior may occur, and lead to unwanted additional frequencies. For that purpose, we modulated the net lateral force at different frequencies ($f_{LF} = 25$, 50 and 75 Hz) and same vibration amplitude ($A_0 = 2.6\mu m$) according to both methods. A finger is pressing at $F_N = 0.3N$. The resulted force in the lateral direction using the 3-axis force sensor is given in Figure 3. Additional harmonics appear on the spectrum of the measurements, but at very low relative amplitude (20% of the fundamental frequency). Therefore, both methods are suitable to create vibrotactile cues at single frequency.

4 Experiment1: Detection threshold

In this experiment, we want to measure the detection threshold of vibrotactile stimulation based on net lateral force. To estimate the threshold and slope of the psychometric function, we are using a weighted and transformed 1-up/2-down staircase.

4.1 Participants

A total of twelve participants were initially recruited for the study. However, one participant was excluded due to experiencing loss of touch on the tip of his fingers. Consequently, the final cohort comprised eleven healthy volunteers, consisting of 8 males and 3 females, with an average age of $M = 30$ and a standard

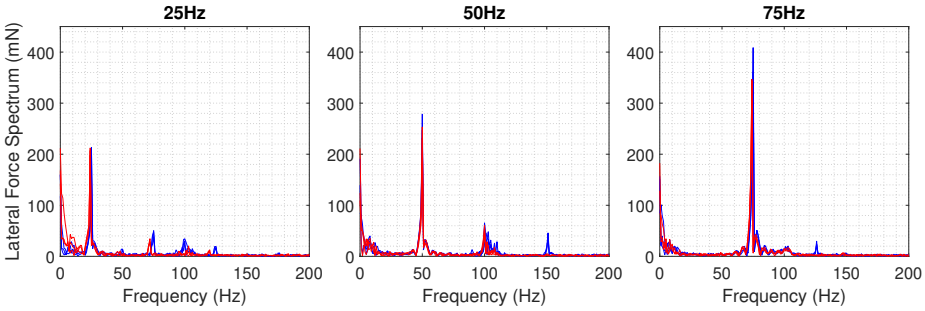

Fig. 3. Spectrum of measured lateral force F_L at $f_{BF} = 25$Hz, 75Hz and 150Hz; AM modulation in blue, PM modulation in red.

deviation of $SD = 9.16$. Among the participants, 10 were right-handed, while one was left-handed. None of the participants exhibited any motor difficulties or sensory impairments in their dominant hand index finger.

Participation in the experiments was voluntary, and informed consent was obtained from each participant prior to the commencement of the study. The experimental procedures were approved by the ethical committee of Lille University, ensuring adherence to ethical standards.

4.2 Stimuli

Our experiment aims to measure the threshold of vibrotactile feedback based on net lateral force. The two aforementioned methods for generating vibrotactile stimulation (AM and PM), are studied at a frequency $f_{LF} = 75$Hz. Each stimulus is presented for a duration of 2 seconds.

4.3 Method

Two experiments were conducted to measure the threshold of vibrotactile stimulation and to estimate the psychometric function of the AM stimuli and PM stimuli, respectively. The primary aim was to assess thresholds across the different experimental conditions using a two-alternative forced-choice paradigm.

Each participant underwent both experiments, and we alternated the order to avoid bias due to the presentation order.

To accomplish this task, we employed a weighted and transformed 1-up/2-down staircase method to present the amplitude at each trial. Employing this algorithm, where the upward step size is three times larger than the downward step size, yields a target probability of $p = 0.866$ [12, 9].

To evaluate the performance of participant responses, a subset consisting of a quarter of the trials was randomly chosen as "phantom" trials. In these phantom trials, the haptic device was not actuated, yet participants were instructed to discern and report whether they perceived a vibration.

4.4 Procedure

In both experimental sessions, participants were comfortably seated in a chair facing the device in a quiet room. To ensure that participants become familiar with the experimental setup, a training session consisting of presenting several stimuli helps to ensure a clear understanding of the task ahead.

Following the training session, participants undertook a forced-choice task. In each trial, they were instructed to apply a specific pressing force to the device, ranging between 0.3 N and 0.4 N. To assist them in maintaining the force throughout the trials, a visual cue based on the force sensor measurement was provided, as depicted in Figure 4. Subsequently, a two-second-long vibration was activated. Upon the vibration's conclusion, participants were tasked with indicating whether they perceived the vibration before advancing to the next trial.

Fig. 4. Visual cue in the form of loading bar that increases with the pressing force (in gramme "gf"). The arrow represent the limit that should not be surpassed.

All the participants performed a total of 100 trials for each experiment. The minimum number of reversal points we achieved with this number of trials during the experiments were 18 (M=23, SD=2.32) and 18 (M=23, SD=2.69) for AM and PM stimuli, respectively. This number ensures a good estimation of the parameters as we run a pretrial test in order to choose the initial value of the staircase to be close to the expected estimated threshold. We chose a random values between 1.2 µm and 1.5 µm for both conditions.

4.5 Data Analysis

The psychophysical curve was estimated with the weighted and transformed 1-up/2-down staircase. We estimate the threshold and slope of each participant in both experiments separately.

A standard function to predict the psychometric function for a forced-choice experiment is the so-called Weibull cumulative distribution function, defined as follows:

$$W(x) = 1 - (1-g)e^{-\frac{k.x}{t}^s}, with\ \ k = -\log\left(\frac{1-a}{1-g}\right)^{\frac{1}{s}} \tag{2}$$

where g is the chance performance, i.e., the expected performance to be achieved by chance, this will be estimated based on the participant's performance

on the phantom trials. t represents the threshold, s the slope of the psychometric function, and a is the performance level or targeted threshold performance (86.6%). Using the log-likelihood algorithm, we estimated the best fitting parameters of the psychometric function [9]. All the data analysis was performed in MATLAB 2022b with the appropriate toolboxes [1]

4.6 Results

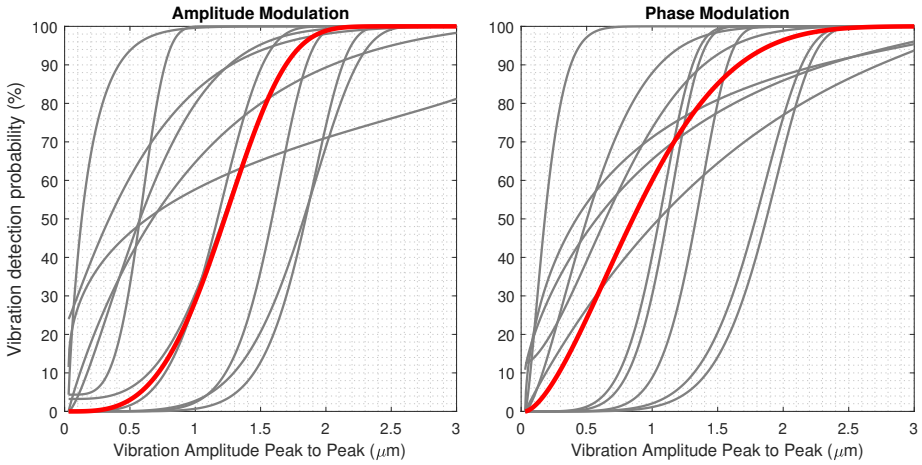

Fig. 5. Vibration discrimination performance using Amplitude Modulation and Phase Modulation. Individual estimated curves are plotted in light gray, and the red curve is based on the median values of threshold and slope (peak to peak vibration amplitude).On the left, the psychometric curve for Amplitude Modulation. On the right, the psychometric curves for phase modulation.

For each participant, we computed the probability of perceiving the vibration. Subsequently, we estimated the best fitting psychometric function in both experiments by maximizing the log-likelihood function. The psychometric functions are represented in figure 5.

For the AM stimuli, the median value of peak to peak threshold and slope estimated were respectively 1.62 µm ($IQR = 1.31-2.02$) and 3.11 ($IQR = 0.95-4.52$) to construct the best-fitting psychometric curve depicted in Figure 5.a. For the PM stimuli, the median value of peak to peak threshold and slope calculated were respectively 1.54 µm ($IQR = 1.28-2.08$) and 1.5 ($IQR = 1.07-6.09$). We illustrate the best-fitting using these parameters in Figure 5.b.

Upon visual inspection of best estimated thresholds of both stimuli, as presented in Figure 6, no distinction between the threshold of both two stimuli is apparent. Additionally, we couldn't find any relation between the same subject threshold in both experiments. To further confirm our observation, we performed

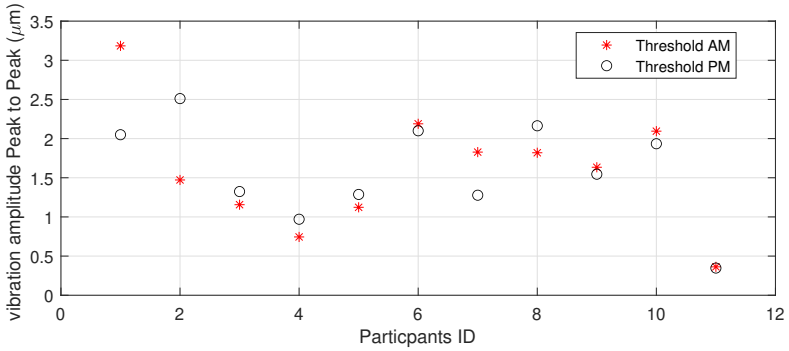

Fig. 6. Best estimated threshold parameters for each participant and both AM stimuli (red stars) and PM stimuli (black circles).

an ANOVA to compare between the thresholds of both stimuli (Figure 7). The analysis shows no statistically significance difference between the thresholds associated with each stimulus.This suggests a comparable impact on perceptual thresholds.

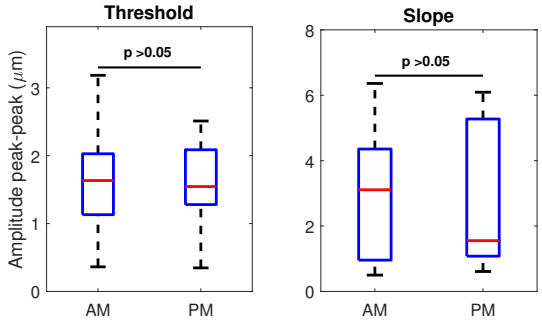

Fig. 7. ANOVA box-plot for threshold and slope for both stimuli.

5 Experiment 2: stimulus intensity comparison with normal vibration

The purpose of this experiment is to map the intensity between the normal and the net shear forces vibrotactile stimuli.

5.1 Stimuli and method

The experimental test bench is completed by a shaker, to which an idle stator of USR60 is attached, in order to preserve the same surface properties, as shown in Figure 8.a.

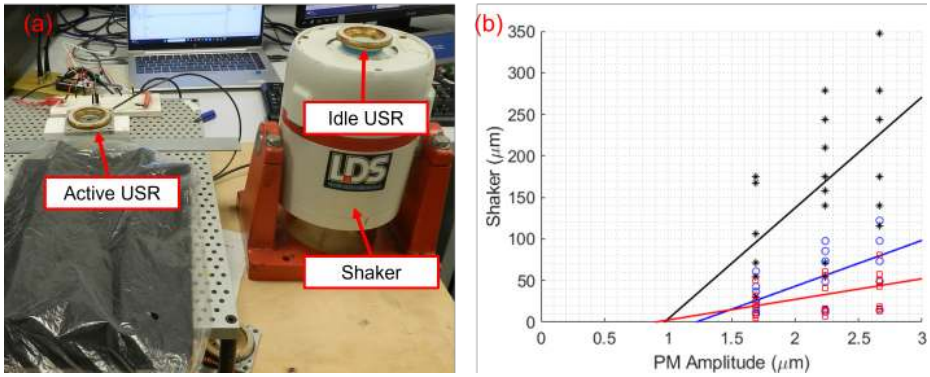

Fig. 8. (a) The experimental setup with an active ultrasonic motor and idle USR placed on the top of the shaker, (b) mapping between normal vibrotactile amplitude and modulated ultrasonic vibration amplitude A_0, for $f_{LF} = 25$Hz in black, $f_{LF} = 75$Hz in blue and $f_{LF} = 150$Hz in red

On the travelling wave stimulator, a constant vibrotactile stimulus is presented using the method denoted as PM, with amplitudes A_0 set to 1.69 µm, 2.23 µm and 2.66 µm, and low-frequency modulation frequencies f_{LF} of 25 Hz, 75 Hz and 150 Hz. Concurrently, the shaker displays a sinusoidal waveform stimulus of the same low frequency as that of the travelling wave modulation frequency. Participants adjust the stimulation amplitude, denoted as A_S, on the shaker to match the perceived stimulus intensity of the travelling wave stimulator. The amplitude of the shaker stimulus is measured using the same laser micrometer employed previously.

At the end of the experimentation, the participants are asked to report about how difficult it was adjusting the level of vibration on the shaker, and which actuator was more comfortable.

Eight participants (5 male, 3 female, with an average age of 29.75 and standard deviation 8.9) participated in the experiment.

5.2 Results

The results are shown in Figure 8.b. Each symbol (circle, square, star) corresponds to an individual answer by a participant. Each particpants data appeared to follow first order polynome. The lines represent the fitted first-order polynomial across all participants and each frequency, and the linear fit is given by:

- $f_{LF} = 25Hz$: $A_S = 133,64(A_0 - 0.99\mu m)$
- $f_{LF} = 75Hz$: $A_S = 55.31(A_0 - 1.21\mu m)$
- $f_{LF} = 150Hz$: $A_S = 24.82(A_0 - 0.89\mu m)$

Moreover, most participants reported that they preferred the modulated net shear forces, because it is more comfortable, in particular at low frequency.

6 Discussion

In this study, we evaluated the sensitivity of vibrotactile stimulation when produced by net lateral force generated by a travelling wave. We estimated the detection threshold for amplitude modulation (AM) or phase modulation (PM) at 75Hz; the most likely parameter value (threshold and slope) show no statistical difference between the two experiments. This result leads us to assume that both methods are similar in terms of vibrotactile sensation. Moreover, Figure 3 indicates no difference in force generation, leading us to infer that vibrotactile sensation may depend more on the force amplitude and frequency rather than the modulation method employed. However, additional work is needed to confirm this trend over a larger span of frequencies.

The value found for the detection threshold is 1.5 µm, and is comparable with the detection threshold obtained with a normal stimulation [14].

However, the results of the second experiment indicate that a much lower vibration amplitude is required for perceiving stimuli with modulated net shear forces generated by the travelling wave compared to normal vibration (shaker). Furthermore, the relationship between A_S (stimulation amplitude) and A_0 (vibrating pot amplitude) seems to be linear. It is noteworthy that one might expect all lines to converge at the origin (0,0); however, interestingly, these lines converge to a point with approximate coordinates of (1 µm, 0). This observation leads to the assumption that the friction mechanisms responsible for creating the net shear forces vanish below a certain vibration amplitude threshold. Indeed, according to [18], a travelling wave can drive objects, including skin, only if there is at least half a wavelength in contact. Therefore, establishing a model of the skin's response to a travelling wave is necessary to further investigate this phenomenon. Additionally, this model would shed light on why the slope of the linear fit depends on frequency.

Finally, the participants reported more comfortable experience with the travelling wave stimulator. Indeed, the device emits no audible noise, even at low frequency, since it is based on ultrasonic vibrations, which represents an advantage over the shaker.

7 Conclusion

Ultrasonic travelling waves have diverse applications in tactile displays, and our paper showcases their effectiveness in delivering vibrotactile cues to a participant's finger. One significant advantage of these devices is their silent operation.

Additionally, they require a significantly lower vibration amplitude compared to traditional vibrations—up to 24 to 155 times lower—to achieve the same perceived stimulus intensity. This reduction in amplitude is pivotal and has the potential to drive technological advancements in vibrotactile stimulators, rendering them more compact, versatile and energy-efficient.

However, the mechanisms responsible for producing the net shear forces are still not fully understood. We hypothesize that there exists a minimal vibration amplitude, below which the travelling wave produces no force on the finger pulp. Further investigations are necessary to confirm or refute this assumption and to elucidate the key factors influencing this minimal vibration amplitude. Establishing a model of force generation would be instrumental in designing future prototypes that exploit ultrasonic travelling waves.

Acknowledgments. This project has received support from the French National Agency for Research (ANR) as part of the project HASAMe under agreement ANR-21-CE33-0020.

This work is supported by IRCICA (Research Institute on software and hardware devices for Information and Advanced Communication, USR CNRS 3380).

The authors acknowledge the use of artificial intelligence for enhancing grammatical accuracy and readability in this work. However, it is important to clarify that the content and ideas presented are solely the creation of the authors. The utilization of AI does not diminish the originality of our work.

Disclosure of Interests. The authors have no competing interests to declare that are relevant to the content of this article

References

1. Alcalá-Quintana, R., García-Pérez, M.A.: Fitting model-based psychometric functions to simultaneity and temporal-order judgment data: Matlab and r routines. Behavior Research Methods **45**, 972–998 (2013)
2. Biggs, J., Srinivasan, M.A.: Tangential versus normal displacements of skin: relative effectiveness for producing tactile sensations. Proceedings 10th Symposium on Haptic Interfaces for Virtual Environment and Teleoperator Systems. HAPTICS 2002 pp. 121–128 (2002), https://api.semanticscholar.org/CorpusID:15300809
3. Cai, Z., Wiertlewski, M.: Ultraloop: Active lateral force feedback using resonant traveling waves. IEEE Transactions on Haptics (2023)
4. Chubb, E.C., Colgate, J.E., Peshkin, M.A.: Shiverpad: A glass haptic surface that produces shear force on a bare finger. IEEE Transactions on Haptics **3**(3), 189–198 (2010)
5. Dai, X., Colgate, J.E., Peshkin, M.A.: Lateralpad: A surface-haptic device that produces lateral forces on a bare finger. In: 2012 IEEE Haptics Symposium (HAPTICS). pp. 7–14. IEEE (2012)
6. Dharma, A.A.G., Oami, T., Obata, Y., Yan, L., Tomimatsu, K.: Design of a wearable haptic vest as a supportive tool for navigation. In: Human-Computer Interaction. Interaction Modalities and Techniques: 15th International Conference, HCI International 2013, Las Vegas, NV, USA, July 21-26, 2013, Proceedings, Part IV 15. pp. 568–577. Springer (2013)

7. Dhiab, A.B., Hudin, C.: Confinement of vibrotactile stimuli in narrow plates: Principle and effect of finger loading. IEEE Transactions on Haptics **13**(3), 471–482 (2020)
8. Garcia, P., Giraud, F., Lemaire-Semail, B., Rupin, M., Kaci, A.: Control of an ultrasonic haptic interface for button simulation. Sensors and Actuators A: Physical **342**, 113624 (2022)
9. Garcıa-Pérez, M.A.: Forced-choice staircases with fixed step sizes: asymptotic and small-sample properties. Vision research **38**(12), 1861–1881 (1998)
10. Ghenna, S., Vezzoli, E., Giraud-Audine, C., Giraud, F., Amberg, M., Lemaire-Semail, B.: Enhancing variable friction tactile display using an ultrasonic travelling wave. IEEE transactions on haptics **10**(2), 296–301 (2016)
11. Gueorguiev, D., Kaci, A., Amberg, M., Giraud, F., Lemaire-Semail, B.: Travelling ultrasonic wave enhances keyclick sensation. In: Haptics: Science, Technology, and Applications: 11th International Conference, EuroHaptics 2018, Pisa, Italy, June 13-16, 2018, Proceedings, Part II 11. pp. 302–312. Springer (2018)
12. Karmali, F., Chaudhuri, S.E., Yi, Y., Merfeld, D.M.: Determining thresholds using adaptive procedures and psychometric fits: evaluating efficiency using theory, simulations, and human experiments. Experimental brain research **234**, 773–789 (2016)
13. Lylykangas, J., Surakka, V., Salminen, K., Raisamo, J., Laitinen, P., Rönning, K., Raisamo, R.: Designing tactile feedback for piezo buttons. In: Proceedings of the SIGCHI Conference on Human Factors in Computing Systems. pp. 3281–3284 (2011)
14. Morioka, M., Whitehouse, D.J., Griffin, M.J.: Vibrotactile thresholds at the fingertip, volar forearm, large toe, and heel. Somatosensory & motor research **25**(2), 101–112 (2008)
15. Pra, Y.D., Papetti, S., Järveläinen, H., Bianchi, M., Fontana, F.: Effects of vibration direction and pressing force on finger vibrotactile perception and force control. IEEE Transactions on Haptics **16**(1), 23–32 (2023). https://doi.org/10.1109/TOH.2022.3225714
16. Storck, H., Wallaschek, J.: The effect of tangential elasticity of the contact layer between stator and rotor in travelling wave ultrasonic motors. International Journal of Non-Linear Mechanics **38**(2), 143–159 (2003). https://doi.org/https://doi.org/10.1016/S0020-7462(01)00048-8, https://www.sciencedirect.com/science/article/pii/S0020746201000488
17. Terenti, M., Vatavu, R.D.: Measuring the user experience of vibrotactile feedback on the finger, wrist, and forearm for touch input on large displays. In: CHI Conference on Human Factors in Computing Systems Extended Abstracts. pp. 1–7 (2022)
18. Wallaschek, J.: Contact mechanics of piezoelectric ultrasonic motors **7**(3), 369 (jun 1998). https://doi.org/10.1088/0964-1726/7/3/011, https://dx.doi.org/10.1088/0964-1726/7/3/011
19. Wiertlewski, M., Lozada, J., Hayward, V.: The spatial spectrum of tangential skin displacement can encode tactual texture. IEEE Transactions on Robotics **27**(3), 461–472 (2011)
20. Zárate, J.J., Shea, H.: Using pot-magnets to enable stable and scalable electromagnetic tactile displays. IEEE transactions on haptics **10**(1), 106–112 (2016)